

The infrapatellar fat pad contributes to spontaneous healing after complete anterior cruciate ligament injury

Takuma Kano^{1,2,3} , Yuki Minegishi^{1,4}, Hidenobu Terada^{1,3}, Chiharu Takasu^{1,3}, Takuma Kojima^{1,2}, Yuichiro Oka⁵, Sora Kawabata¹, Naoki Shimada¹, Yuri Morishita⁶, Kenji Murata⁷ and Naohiko Kanemura⁷

¹Department of Health and Social Services, Graduate School of Saitama Prefectural University, Saitama 343-8540, Japan;

²Soka Orthopedic Internal Medicine, Saitama 340-0016, Japan; ³Yatsuka Orthopedic Internal Medicine, Saitama 340-0028, Japan;

⁴Department of Rehabilitation, Faculty of Health Sciences, Nihon Institute of Medical Science, Saitama 350-0435, Japan;

⁵Faculty of Health Sciences, Hokkaido University, Sapporo 060-0812, Japan; ⁶Tokyo Kasei University, Sayama 350-1398, Japan;

⁷Saitama Prefectural University, Saitama 343-8540, Japan

Corresponding author: Naohiko Kanemura. Email: kanemura-naohiko@spu.ac.jp

Impact Statement

Anterior cruciate ligament (ACL) injuries are a frequent lower extremity joint trauma, and surgical reconstruction is the gold standard for ACL treatment. Rodent studies have reported that the ACL spontaneous healing model controls abnormal anterior tibial translation after injury and achieves spontaneous healing. However, the detailed mechanisms leading to the spontaneous healing of complete ACL tears are still unknown. In this study, we focused on the dynamics of the intra-articular knee tissues during the acute phase of ACL injury and revealed part of the healing mechanisms. Our results indicate the possibility of conservative treatment for patients with complete ACL injury based on the assumption of spontaneous healing and contribute to the development of regenerative medicine and drug research to establish conservative treatment methods for ACL injury in the future.

Abstract

Anterior cruciate ligament (ACL) injuries have a very low healing capacity but have recently been shown to heal spontaneously with conservative treatment. This study examined the mechanism of spontaneous ACL healing by focusing on the intra-articular tissues of the knee joint. Skeletally mature Wistar rats ($n = 70$) were randomly assigned to two groups: the controlled abnormal movement (CAM) and anterior cruciate ligament transection (ACLT) groups. The ACL was completely transected at the mid-portion in both groups. Only the CAM group underwent extra-articular bracing to control for abnormal tibial translation. The animals were allowed full cage activity until sacrifice for histological, and molecular biology analyses. The results showed that the behavior of the stump after ACL injury differed between models 12 h after injury. The femoral stump in the ACLT group retreated posteriorly and upwardly. Macrophage polarity analysis revealed that the stump immune response in the CAM group was more activated than that in the ACLT group 6 h after injury. Microarray analysis of the ACL parenchyma and infrapatellar fat pads suggested the involvement of nuclear factor kappa B (NF- κ B) signaling. Real-time polymerase chain reaction (PCR) analysis showed that *NF- κ B* gene expression in the infrapatellar fat pad was significantly increased in the CAM group than in the ACLT group. However, there was no difference in the gene expression levels in the ACL parenchyma between models. In conclusion, the healing response of the ACL

was activated within 12 h of injury, resulting in differences in the healing response between the models. It has been suggested that infrapatellar fat pads are involved in the healing process and that angiogenesis and antiapoptotic effects through NF- κ B signaling may contribute to this mechanism.

Keywords: Anterior cruciate ligament, spontaneous healing, NF- κ B, infrapatellar fat pads, angiogenesis, macrophage

Experimental Biology and Medicine 2023; 248: 1895–1904. DOI: 10.1177/15353702231215921

Introduction

More than 120,000 ACL injuries occur annually in the United States.^{1,2} Although surgical reconstruction using autologous tendons is the gold standard in ACL treatment, approximately half of patients with ACL injuries opt for conservative

treatment.¹ However, the ability of the ACL to heal spontaneously is very poor,^{3–9} and conservative therapy could not spontaneously heal the ruptured ACL.^{1,10} A new model called the controlled abnormal movement (CAM) model controls abnormal tibial anterior translation after injury from outside the joint capsule in rodent studies and has reportedly

achieved spontaneous healing.^{11–14} In this model, the mechanical properties of the healed ACL, regardless of the injury site, were approximately 50% of those of a normal ligament.¹¹ This study showed the possibility of conservative treatment based on the assumption of spontaneous ACL healing in patients with ACL injuries. In clinical research, Ihara and Kawano¹⁵ and Ihara *et al.*¹⁶ reported that spontaneous healing of the damaged ACL was achieved by conservative treatment with bracing treatment in patients with a completely ruptured ACL. However, there have been only a few reports on the spontaneous healing of completely injured ACLs, and the detailed mechanisms leading to the spontaneous healing of complete ACL tears are still unknown.

Blood supply is essential to repair connective tissue. Its importance has been reported in Achilles tendon and knee medial collateral ligament injuries.^{5,17,18} Hypoangiogenesis reduces the supply of oxygen, growth factors, and other metabolically essential nutrients, delaying ligament binding or nonunion. Morishita *et al.*¹³ and Nishikawa *et al.*¹⁴ performed molecular biological analyses at one-, three-, and five-day intervals after ACL injury and reported decreased mRNA expression of the catabolic factor matrix metalloproteinase-13. They also found an increased expression of platelet-derived growth factor (PDGF)- β mRNA in the CAM model compared to the anterior cruciate ligament transection (ACLT) group. They further identified differences in the catabolic balance (matrix metalloproteinase-13/tissue inhibitor of metalloproteinase-1) between the models.^{13,14} One day after ACL injury, in the CAM model, histological changes induced the connection between the ACL stump and intra-articular tissue (infrapatellar fat pad/synovial tissue). However, in the ACLT model, an upward and backward regression of the injured ACL stump was observed.^{11,13,14} These reports suggest that within 24 h after an ACL injury, the CAM–ACLT model shows a difference in the molecular mechanism underlying the healing response of the ACL parenchyma and the histological behavior of the injured ACL stump. Moreover, intra-articular tissues are involved in cross-linking between stumps after ACL injury. These phenomena suggest that the inflammatory response was activated within 24 h after ACL injury and that the ACL parenchymal and intra-articular tissues may have exhibited complementary repair mechanisms to achieve spontaneous healing of the ACL.

This study hypothesized that intra-articular tissues contribute to the ACL injury healing mechanism through cross-linking and improving blood flow supply at the ACLT. This study aimed to elucidate the mechanism of spontaneous healing of injured ACL by analyzing the dynamics of the stump and intra-articular tissue in the acute phase of ACL injury. Elucidating this mechanism may provide evidence for new treatment strategies to promote spontaneous ACL healing and ensure the reproducibility of treatment outcomes.

Materials and methods

Experimental design

All experiments were approved by the University Animal Experiment Ethics Committee (permit no. 2021-7) and were performed in accordance with the Guidelines for the Care and Use of Laboratory Animals. Seventy mature, 12-week-old male Wistar rats weighing 260–310 g (Japan SLC, Shizuoka, Japan)

were used (Figure 1). Rats were randomly assigned to one of the following groups: CAM and ACLT. The animals were allowed full cage activity, and the room temperature was maintained at $23 \pm 2^\circ\text{C}$ with a 12-h light–dark cycle. To clarify the spontaneous ACL healing response in the acute phase, the CAM and ACLT groups were compared histologically at 1, 3, 6, 12, and 24 h, and three days postoperation ($n=5$, each group); using molecular biology techniques at 12 h ($n=7$, each group); and via microarray analysis ($n=2$, each group), real-time polymerase chain reaction (PCR) analysis ($n=5$, each group), and vascular morphology analysis at seven days ($n=1$, each group). To clarify the spontaneous healing response of the ACL in the acute phase, the CAM and ACLT groups were compared histologically at 1, 3, 6, 12, and 24 hours and 3 days after surgery ($n=5$, each group); real-time polymerase chain reaction (PCR) analysis ($n=5$, each group).

Surgical procedures

The surgical procedures were performed as described in a previous study.¹⁰ Briefly, the animals were anesthetized via intraperitoneal injection with a combination anesthetic comprising medetomidine (0.375 mg/kg), midazolam (2.0 mg/kg), and butorphanol (2.5 mg/kg). A parapatellar arthrotomy was performed on the left hind limb to expose the anterior ACL. For the ACLT and CAM groups, scissor blades were inserted into the joint capsule, and the ACL was transected at the mid-portion. The joint capsule and parapatellar fascia were then closed with running sutures. Next, a 1-mm diameter steelhead was drilled into the medial aspect of the tibial tuberosity in the mediolateral direction. Precise positioning of this bone hole was critical to avoid the patellar tendon and joint capsule, but it should still penetrate a sufficient amount of bone. To control anterior tibial translation, a double 3-0 nylon suture was placed through the tibial bone hole posterior to the condyle of the distal end of the femur and was tied to the joint to prevent anterior tibial translation. The skin was closed using running and interrupted sutures. In the ACLT group, the same procedure was performed until the dual 3-0 nylon suture was placed through the tibial ostia behind the condyle at the distal end of the femur; however, for this group, we did not control anterior tibial movement. All animals were allowed unrestricted cage movement immediately after the surgery.

Histological evaluation

The intra-articular tissue healing response of the knee joint was evaluated histologically at 1, 3, 6, 12, and 24 h, and three days postsurgery. Knee joints were harvested from five animals in each group and fixed in 4% paraformaldehyde at each time point. After fixation, all tissues were decalcified in 10% ethylenediaminetetraacetic acid in phosphate-buffered saline (PBS) (pH=7.4) at 4°C for five to six weeks. Tissues were infiltrated with PBS containing sucrose at 4°C and embedded in an optimal cutting temperature compound for flash freezing (Sakura Finetek Japan, Tokyo, Japan). Longitudinal cryosections (14 mm thick) along the sagittal plane were obtained, mounted on slides, and maintained at -80°C . Cryosections were stained with hematoxylin and eosin (H&E) to observe the general and macroscopic morphological characteristics of the ruptured ACL. Oil Red O staining was performed to assess the localization of the infrapatellar fat pad.

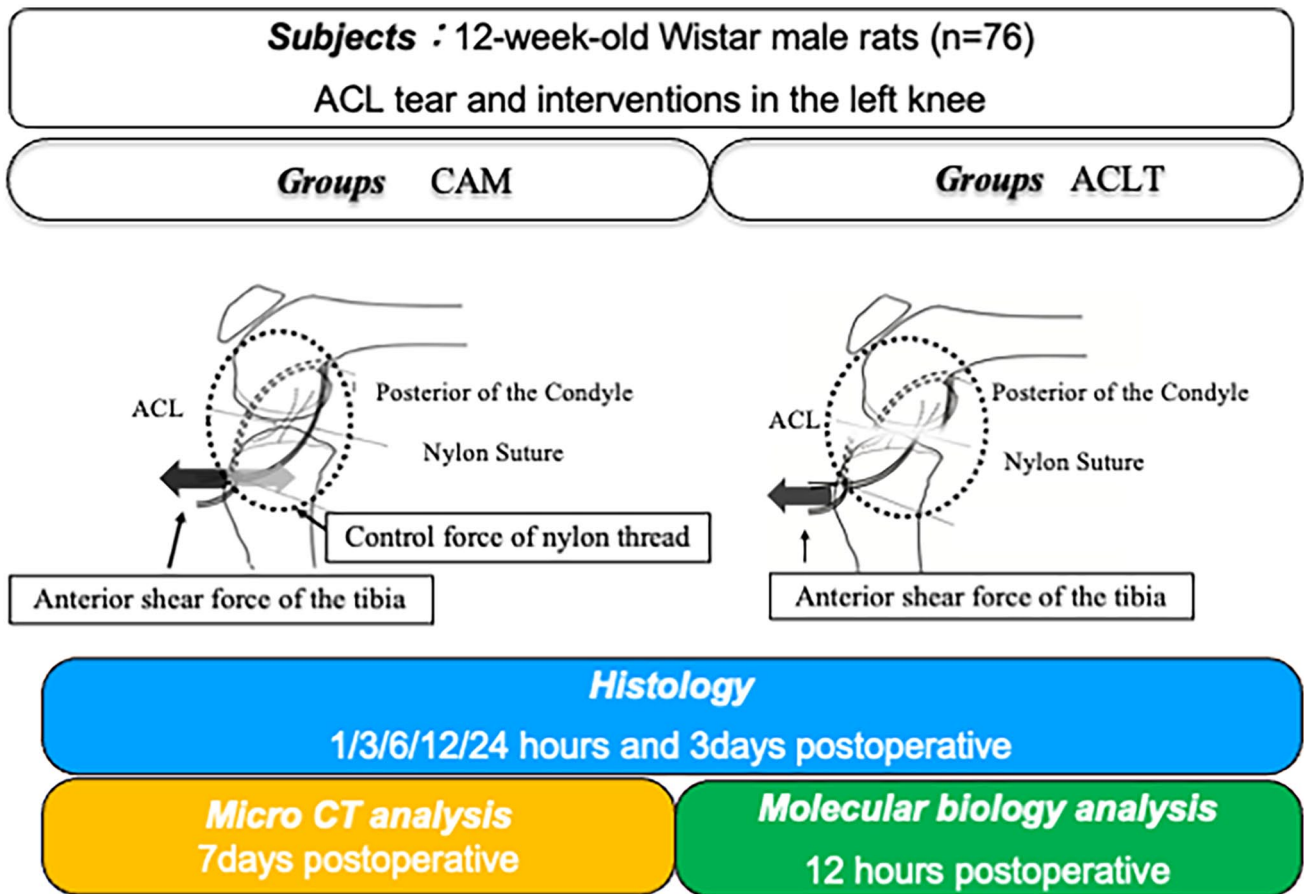


Figure 1. Flowchart showing the allocation of rats in the study. (A) CAM, controlled abnormal movement model. (B) ACLT, anterior cruciate ligament transection.

Immunohistochemistry staining

Immunohistochemical staining was performed to detect hypoxia-inducible factor (HIF)-1 α , α -SMA, CD68, and CD206 at 1, 3, 6, 12, and 24 h, and three days after injury. Anti-HIF-1 α antibodies were used to assess hypoxia in the cells, while anti-CD68 and anti-CD206 antibodies were used to evaluate the immune response. The slides were dried at room temperature (24°C) for approximately 30 min, followed by immunohistochemistry (IHC) staining to determine protein localization. The primary antibodies used were (PBS-diluted): anti-HIF-1 α rabbit polyclonal antibody (dilution ratio 1:1000, BS-0737R; Bioss, Woburn, MA, USA), anti- α -SMA rabbit polyclonal antibody (dilution ratio 1:1,000, GTX100034; GeneTex, Irvine, CA, USA), anti-NF- κ B p65 antibody (dilution ratio 1:500, GTX102090, GeneTex), anti-CD68 rabbit polyclonal antibody (dilution ratio 1:1,000, ab125212; Abcam, Cambridge, England), and anti-CD206 rabbit polyclonal antibody (dilution ratio 1:1,000, 18704-1-AP; Proteintech, Rosemont, IL, USA). Goat-derived antirabbit IgG antibody was used as the secondary antibody (Vector Laboratories, Burlingame, CA, USA). For the sensitization reaction, the avidin-biotinylated enzyme complex method was performed using a VECTAIN ABC Rabbit IgG Kit (Vector Laboratories). A SAB-POI kit (DAB) (Nichirei Bioscience Inc., Tokyo, Japan) was used. Nuclear counterstaining was performed using hematoxylin. PBS was used as the negative control. To calculate the CD206-to-CD68 positivity rate, five regions were

randomly selected from the femoral and tibial stumps. The number of CD68- and CD206-positive cells relative to the total number of cells in each region was calculated to determine the CD206-to-CD68 positivity rate.

Real-time PCR

ACL and infrapatellar fat pad samples from the ACLT and CAM groups were evaluated for mRNA expression using real-time PCR 12 h postsurgery. The relative expression levels of target genes were calculated using the $2^{-\Delta\Delta Ct}$ method. The ACL parenchyma and infrapatellar fat pad of the ACLT group were used for standardization. Real-time PCR was performed using a StepOnePlus real-time system (Applied Biosystems, Foster City, CA, USA). Primers were selected from the following NF- κ B signal-related factors: interleukin 1 receptor, type I (IL1R; Rn00565482_m1), tumor necrosis factor receptor (TNFR) (Rn01492828_g1), HIF-1 α (Rn01472831_m1), NF- κ B (Rn00595794_m1), or vascular endothelial growth factor A (VEGF-A; Rn01511602_m1).

Statistical analysis

All statistical analyses were performed using Jamovi (version 1.6.23.0; <https://www.jamovi.org/>). Student's *t*-test was used for histological and molecular biological data that showed normality and equal variance. The Wilcoxon rank-sum test was used for data that did not show a normal distribution. The significance level was set at $P=0.05$.

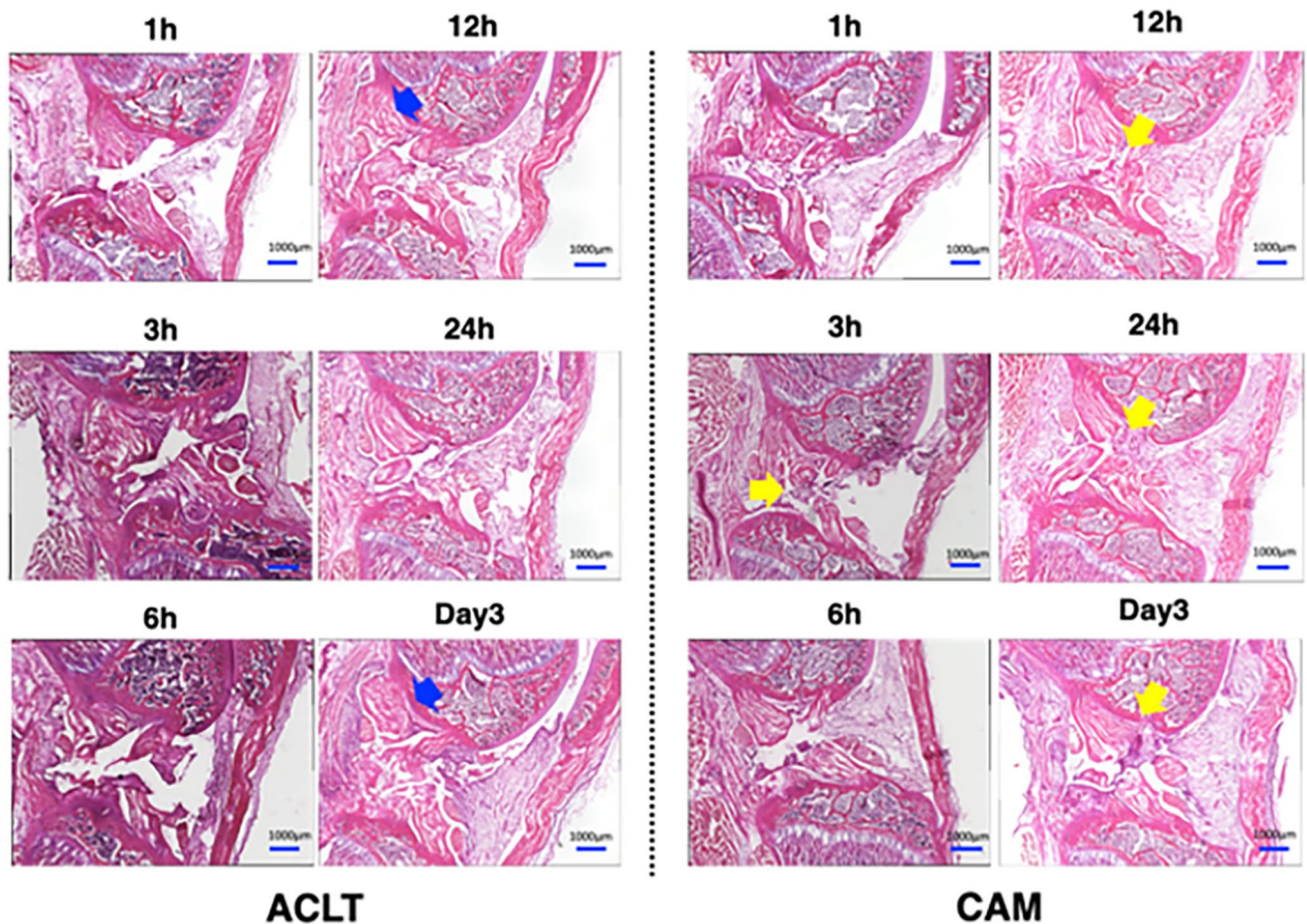


Figure 2. Dynamic changes in the ACL transection in the acute phase of ACL injury.

The dynamic changes in the ACL transection after ACL injury are shown in the hematoxylin/eosin-stained histological images. Blue arrows: tissue image of the posteriorly retracted lateral femoral end of the ACL in the ACLT group. Yellow arrows: intra-articular tissue invasion into the gap between the ACL in the CAM group. Scale bar: 1000 μm .

Results

Histological analysis

The remnants of the transected ACL in the CAM group appeared to be in relatively closer proximity at three days postinjury compared to the ACLT group. From 1 to 24 h post-ACLT, infrapatellar fat pads were observed to proliferate and fill the gap. In contrast, in the ACLT group, the ACL femoral residuals retracted posteriorly, and the intertrochanteric distance widened at 12 h postinjury. Infrapatellar fat pads were observed to invade the ACLT at 3 h postinjury but were not observed to localize after that (Figures 2 and 3).

Immunohistochemical staining showed that HIF-1 α was activated in the injured ACL remnants in both the CAM and ACLT groups (Figure 4). In both groups, cells in the stump showed intense staining for α -SMA from the early stage of injury, and this trend continued until three days postsurgery (Figure 5). There was a considerably significant difference between the number of CD68-positive and CD206-positive cells in the femoral/tibial side remnant of the injured ACL (Figure 6). The CD68-to-CD206 positivity ratio in the femoral side remnant was 70.8 [67.2–72.3] in the CAM group and 57.9

[56.7–60.0] in the ACLT group ($P=0.01$) at 6 h after injury; CAM group: 94.6 [88.8–96.6], ACLT group: 31.2 [30.2–33.8] ($P<0.01$) at 12 h; and CAM group: 95.7 [64.4–96.1], ACLT group: 54.6 [20.7–66.8] ($P<0.01$) at 24 h postinjury. The CD68-to-CD206 positivity ratio in the tibial side remnant of the CAM group was 75.0 [68.0–80.7], while that of the ACLT group was 45.0 [43.2–49.2] ($P<0.01$) at 6 h after injury; CAM group: 92.1 [90.9–98.6], ACLT group: 74.7 [72.0–75.6] ($P<0.01$) at 12 h; and CAM group: 97.4 [96.6–97.8], ACLT group: 61.6 [56.4–67.1] ($P<0.01$) at 24 h (Table 1). NF- κ B showed staining in the CAM group at the ACLT and in the sub patellar fat body, but not in the ACLT group (Figures 7 and 8).

Real-time PCR analysis

To investigate the differences in biological responses in the ACLT parenchyma and infrapatellar fat pad of each group, we compared the expressions of interleukin 1 receptor type I, TNFR, and HIFs. The relative mRNA expression levels of HIF-1 α , NF- κ B, and VEGF-A in the ACL parenchyma were compared. There was no significant difference in the mRNA expression levels of all factors between the ACL parenchyma of the CAM and ACLT groups. In the infrapatellar fat pad,

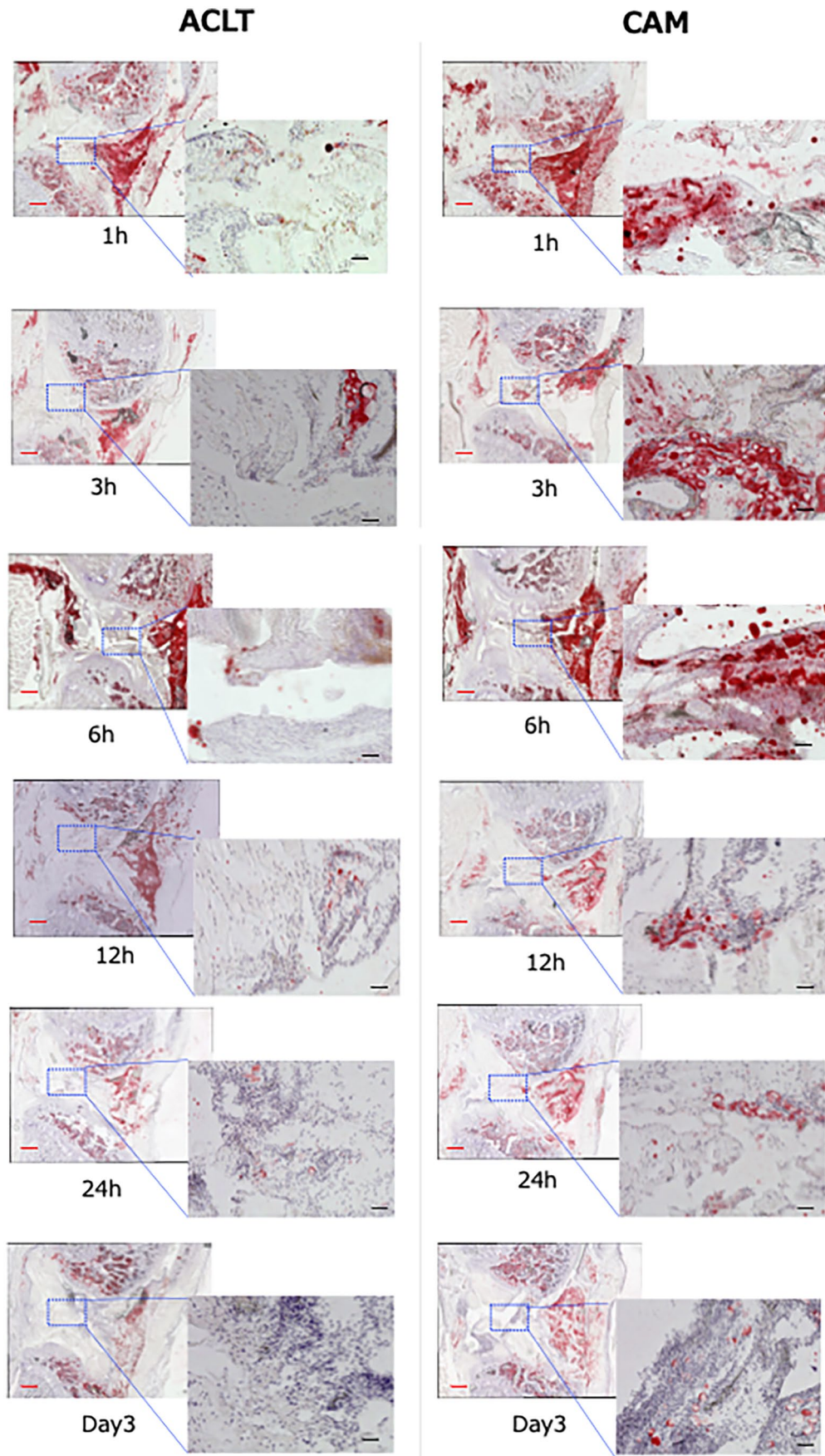


Figure 3. Localization of the fat body under the patella in the acute phase of ACL injury. Also shown is the localization of the infrapatellar fat pad after ACL injury. Scale bars: black, 50 μ m; red, 500 μ m.

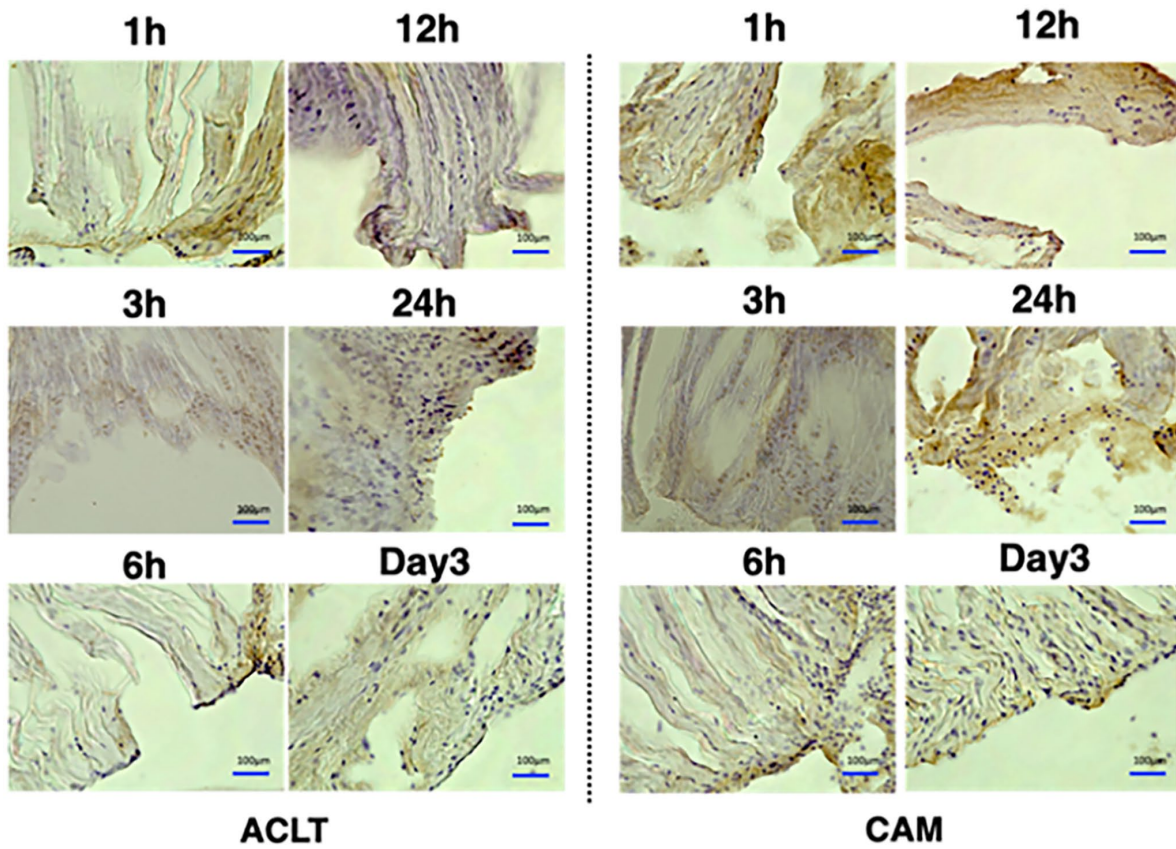


Figure 4. Hypoxia-inducible factor (HIF)-1 α IHC staining image of the lateral femoral dissection after ACL injury. There were no significant differences in cell staining between groups from 1 h after injury. Scale bar: 100 μ m.

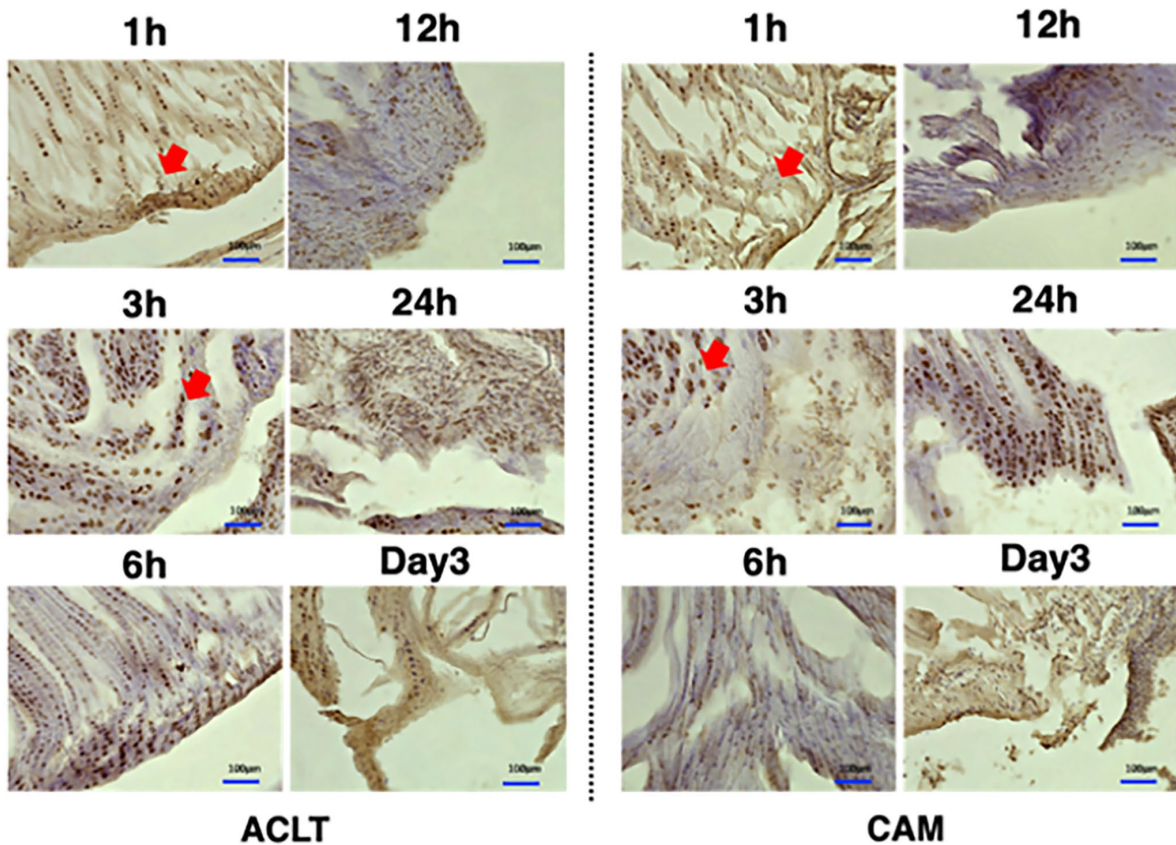


Figure 5. α -SMA IHC staining image of the lateral femoral fragment after ACL injury. A high-cell positivity rate was observed immediately after the injury in both the ACLT and CAM groups (red arrows). Scale bar: 100 μ m. The upper right panel shows the analyzed area (the femoral lateral transection is shown, with a line drawn along the transected margin).

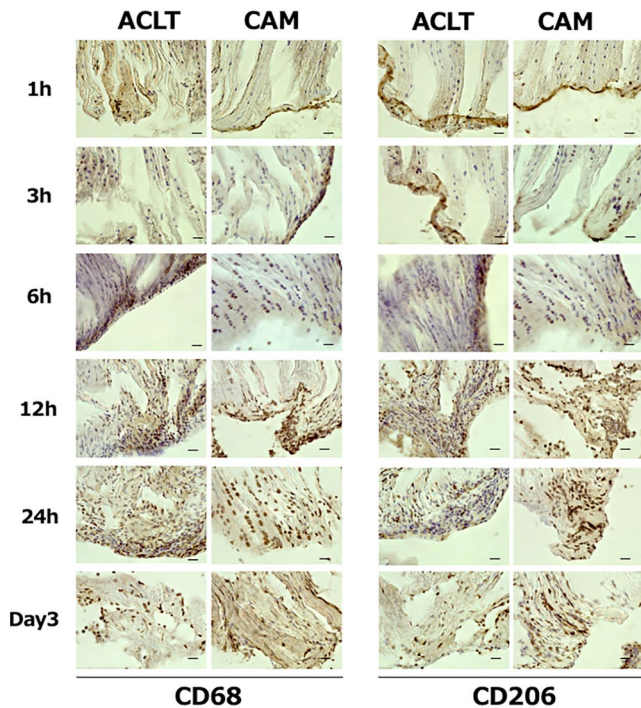


Figure 6. Macrophage ($M\phi$) polarity at the lateral femoral epiphysis after ACL injury. IHC staining images of the $M\phi$ -specific marker CD68 and $M2\phi$ -specific marker CD206 are shown. The nuclei of CD68+ and CD206+ cells become darker in the CAM group and unstained (purple) in the ACLT group with time. Black arrows: positive cells. Scale bar: 50 μ m.

HIF-1 α and *NF- κ B* mRNA expressions were predominantly increased in the CAM group compared to that in the ACLT group ($P=0.038$ and $P<0.001$, respectively) (Figure 9).

Discussion

In this study, we found differences between the models regarding the CD206-positive cell rate in ACL tears at 6h postinjury and the behavior of the ACL tears at 12h postinjury. The differences in the healing responses in the knee joint within 12h after ACL injury may be related to the spontaneous healing ability of the injured ACL. Specifically, the CAM group showed localization of adipose tissue in the ACL stump gap, whereas the ACLT group did not. Therefore, the involvement of the infrapatellar fat pad tissue in the ACL joint was suggested as a factor that caused differences in the ACL healing response between models. Shook *et al.*¹⁹ reported that the adipose tissue depolarizes during wound healing, releases fatty acids that promote macrophage ($M\phi$) activity, and then migrates to the wound site to differentiate into myofibroblasts, promoting wound healing. Myofibroblasts are also abundant during the healing process of the medial collateral ligament of the knee and play an essential role in ligament repair by transmitting contractile force to the initial granulation tissue to promote wound closure.^{7,20,21} Considering the observation of $M\phi$ activity in the ACLT area and the high number of α -SMA-positive cells in the ACLT area in this study, it is possible that the migration of infrapatellar fat pad-derived adipose

tissue to the ACLT area in the knee joint after ACL injury promotes ACL healing.

In addition, mesenchymal stem cells (MSCs), which are abundant in the infrapatellar fat pad within the knee joint capsule after ACL injury,²² have been reported to promote macrophage polarity to the M2 type.²³ It is possible that MSCs also acted on ACL tears in this study, leading to immune response activation. In addition, regarding the blood supply to the injury site, the migration of adipose tissue derived from the infrapatellar fat pad may promote ACL healing. Although the poor vascularization of tissues has been implicated as a cause of ACL healing failure in a previous study using the CAM model,⁵ we observed that injured ACLs did not reattach to each other but to the intra-articular knee tissue (infrapatellar fat pad/synovial tissue).¹¹ The infrapatellar fat pad has abundant capillaries and may alternatively supply blood flow to the injured ACLT. Molecular biological analysis of the infrapatellar fat pad at 12h after ACL injury revealed that the mRNA expression of *NF- κ B*, which is involved in inflammation and angiogenesis, and *HIF-1 α* was significantly increased in the CAM group, suggesting that the infrapatellar fat pad may play an alternative role in affecting blood flow to the ACLT. The infrapatellar fat pad may also be responsible for angiogenesis, blood flow, and nutrient supply to the ACLT.

The ACLT group did not show adipose tissue invasion between ACL transects, whereas the CAM and ACLT groups maintained a higher percentage of CD206-positive cells on the tibial side than on the femoral side. On the contrary, in the CAM group, there was no difference between the tibial and femoral ends. In a previous study on the healing ability of the ACL, the mechanical strength of the ACL was superior in the central ACL injury model.¹¹ However, both angiogenesis²⁴ and cellular activity²⁵ were increased in the proximal femur compared to the central ligament. Based on these events, the infrapatellar fat pad tissue may migrate and act on the transected area depending on the distance between the femoral and tibial sides of the transected area. In a previous study, the ACLT model showed a significant increase in anterior tibial displacement compared with the CAM model.²⁶ In the ACLT model, when the distance between the infrapatellar adipose pad and the lateral femoral transection is extended, adipose tissue cannot migrate, which may lead to the apoptosis of ACL fibroblasts, resulting in the failure of healing.

The molecular biological analysis did not detect any differences in gene expression in the ACL parenchyma. Previous *in vitro* studies examining the cellular activity and proliferative capacity of ACL and medial collateral ligament cells have often pointed out the lack of healing ability of ACL cells.²⁷⁻³⁰ However, the results of this study suggest that there is no direct relationship between the "healing ability of the ACL parenchyma itself" and "whether the injured ACL heals or not" and that conservative healing of the ACL is achieved through the mediation of the braking of abnormal joint motion caused by ACL injury and the infrapatellar fat pad.

There are several points to consider when interpreting the results of this study. First, the ACL injury method does not mimic clinical injury. In a clinical situation, the ACL is

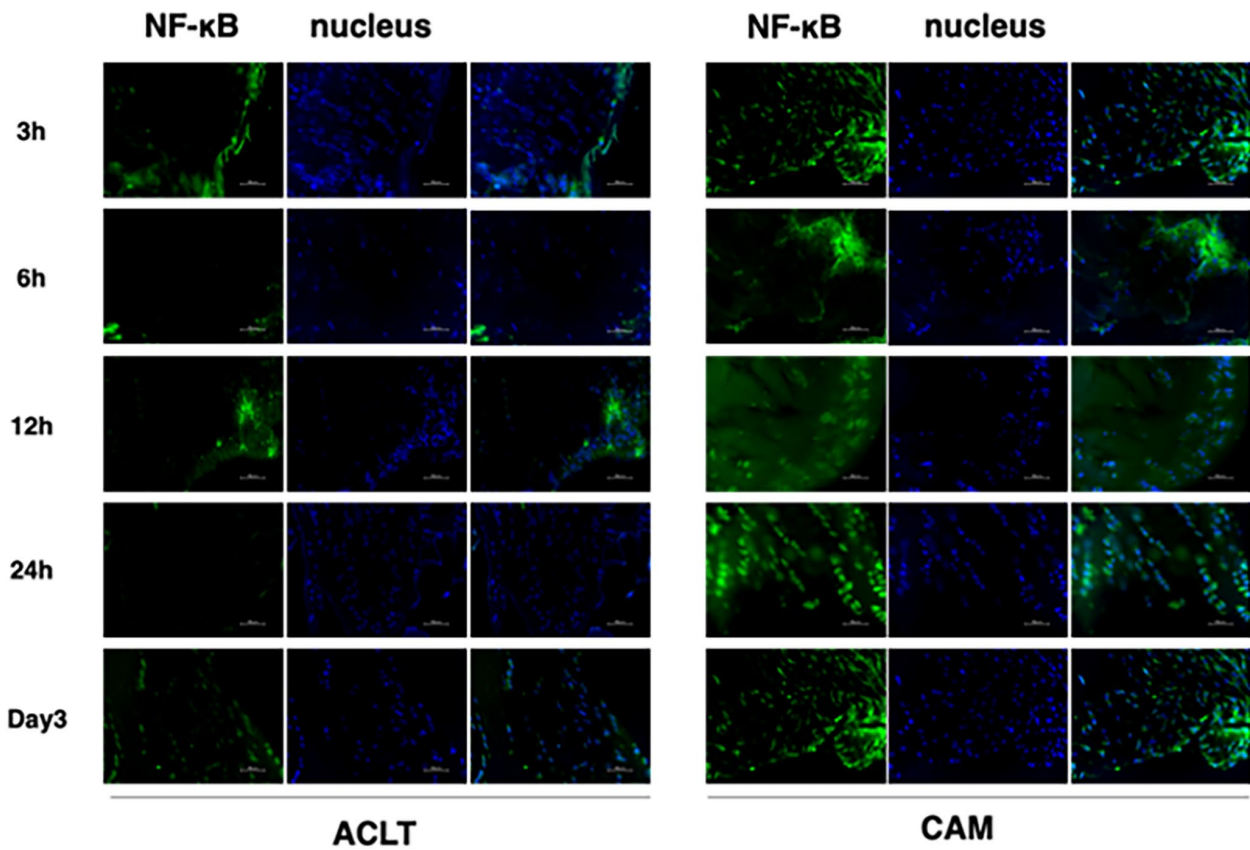


Figure 7. Immunofluorescent staining for NF- κ B and nuclei in the region of ACL injury. (Left column/middle row) Each image. (Right column) Integrated image. Scale bar: 50 μ m.

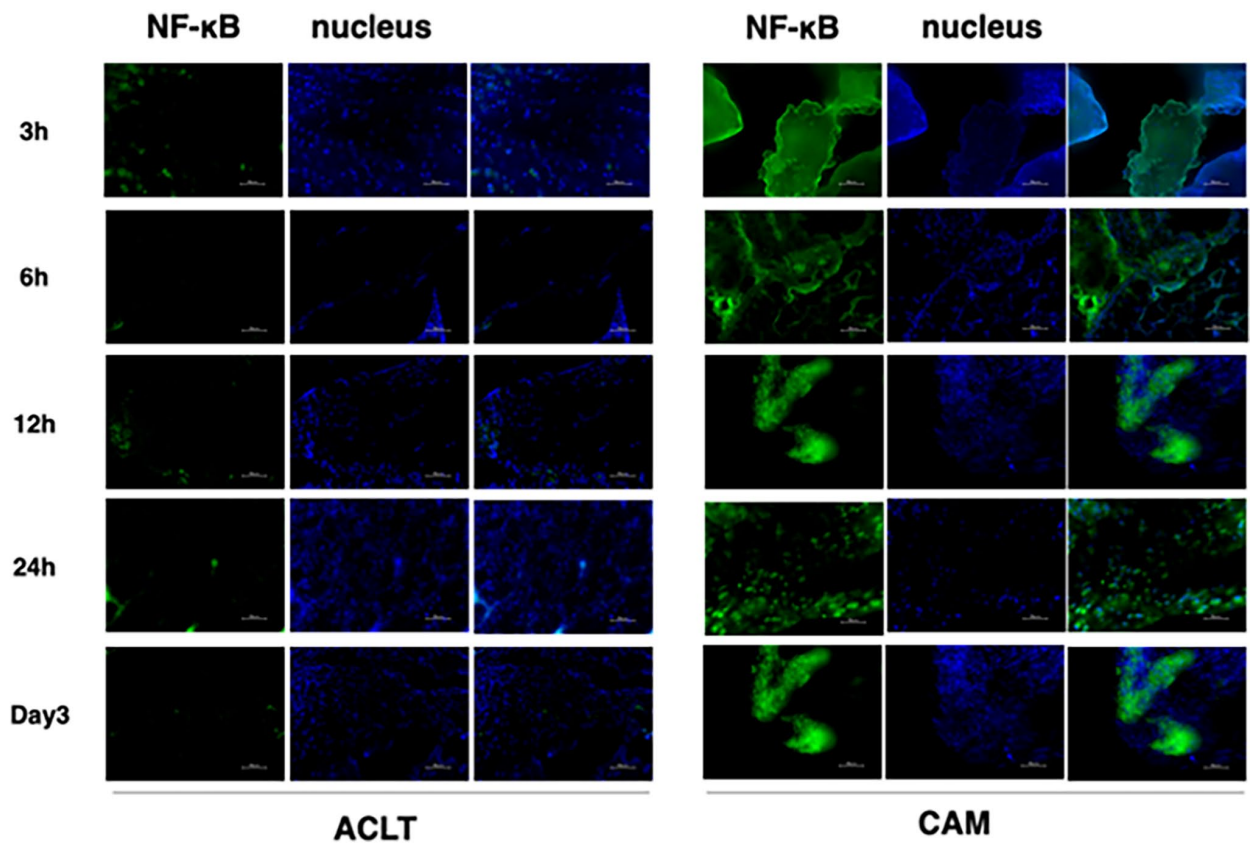


Figure 8. Immunofluorescent staining for NF- κ B and nuclei in the infrapatellar fat pad region. (Left column/middle row) Each image. (Right column) Integrated image. The bar is 50 μ m.

Table 1. Temporal changes in Mφ polarity at the transected edge of each model after ACL injury are shown; the percentage of CD206-positive cells relative to CD68 was significantly higher in the CAM group.

			CD68		CD206		Ratio
			Total cell count	Positive cell count	Total cell count	Positive cell count	CD206-positive cells to CD68-positive cells
3h postinjury	Femoral remnant	ACLT	68.4 ± 26.3	13.4 ± 11.0	75.2 ± 45.7	3.2 ± 2.0	30.5% ± 8.2%
		CAM	61.0 ± 36.4	9.2 ± 8.9	62.6 ± 37.8	3.0 ± 3.0	36.7% ± 7.2%
	Tibial remnant	ACLT	68.8 ± 21.8	11.4 ± 5.2	67.2 ± 13.1	4.2 ± 1.6	41.8% ± 15.7%
		CAM	40.0 ± 16.6	8.2 ± 6.6	41.6 ± 15.5	3.0 ± 1.1	43.3% ± 9.2%
6h postinjury	Femoral remnant	ACLT	210.8 ± 34.7	51.0 ± 9.4	190.2 ± 65.1	26.2 ± 8.4	58.1% ± 1.9%
		CAM	129.2 ± 35.3	55.8 ± 8.3	117.2 ± 25.3	38.2 ± 9.7	73.3% ± 9.0%
	Tibial remnant	ACLT	89.0 ± 51.9	35.0 ± 21.8	90.0 ± 23.8	15.2 ± 5.3	44.4% ± 5.4%
		CAM	80.0 ± 38.0	39.2 ± 23.0	72.0 ± 26.9	27.6 ± 16.8	74.7% ± 8.7%
12h postinjury	Femoral remnant	ACLT	191.0 ± 77.5	81.2 ± 25.6	143.6 ± 159.1	21.0 ± 26.2	31.3% ± 12.8%
		CAM	137.2 ± 87.0	131.2 ± 83.9	178.2 ± 84.3	156.4 ± 71.4	92.9% ± 3.5%
	Tibial remnant	ACLT	81.8 ± 41.6	55.2 ± 30.9	128.6 ± 48.4	60.2 ± 21.6	73.9% ± 3.8%
		CAM	63.6 ± 59.6	60.2 ± 56.9	88.8 ± 72.7	76.6 ± 57.4	94.2% ± 4.0%
24h postinjury	Femoral remnant	ACLT	167.4 ± 138.4	68.4 ± 46.7	153.6 ± 89.1	28.8 ± 13.0	47.7% ± 23.2%
		CAM	107.4 ± 31.4	103.6 ± 30.5	144.0 ± 47.2	130.0 ± 38.0	94.5% ± 2.7%
	Tibial remnant	ACLT	119.6 ± 28.2	72.6 ± 23.3	132.4 ± 43.5	51.4 ± 28.6	57.3% ± 18.5%
		CAM	76.2 ± 21.9	74.2 ± 22.3	76.4 ± 34.2	72.4 ± 32.9	97.3% ± 0.9%
Three days postinjury	Femoral remnant	ACLT	97.8 ± 29.7	89.6 ± 26.0	80.6 ± 41.0	40.2 ± 18.5	56.3% ± 6.4%
		CAM	96.4 ± 22.6	69.0 ± 12.2	114.4 ± 33.6	72.2 ± 19.4	87.5% ± 4.7%
	Tibial remnant	ACLT	107.4 ± 39.3	101.8 ± 37.6	91.4 ± 33.0	61.8 ± 14.9	74.6% ± 16.3%
		CAM	79.6 ± 45.1	66.2 ± 32.3	125.6 ± 36.5	100.6 ± 31.7	90.9% ± 3.3%

ACL: anterior cruciate ligament; ACLT: anterior cruciate ligament transection; CAM: controlled abnormal movement.

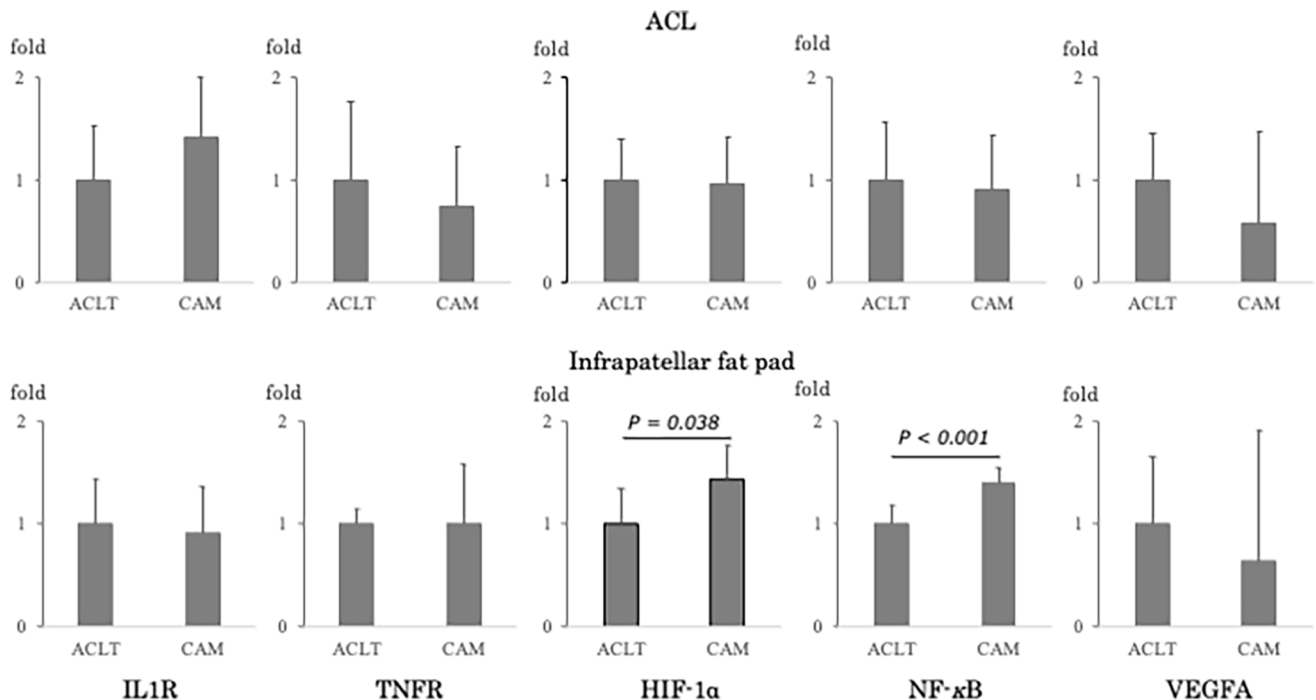


Figure 9. Relative gene expression levels at 12h postinjury. Differences in *HIF-1α* and *NF-κB* mRNA expressions in the infrapatellar fat pad were observed between models. (A) Gene expression levels in the ACL parenchyma. (B) Gene expression levels in the infrapatellar fat pad. All data are presented as the mean ± SD (Vertical axis unit: fold change).

torn owing to abnormal extension stress on the knee joint. Second, because this study was an *in vivo* experiment, the interpretation of the interaction between the ACL parenchyma and subacetabular fat body during the healing process is limited. Additional *in vitro* studies are required to verify these findings.

AUTHORS' CONTRIBUTIONS

TK conceived the idea for this study. YM, YM, and SN contributed to the establishment of the model. HT, CT, TK, YO, and SK contributed to the interpretation of histology and molecular biology results. NK and KM oversaw the conduct of the study. All authors approved the final version of the manuscript for publication.

DECLARATION OF CONFLICTING INTERESTS

The author(s) declared no potential conflicts of interest with respect to the research, authorship, and/or publication of this article.

FUNDING

The author(s) disclosed receipt of the following financial support for the research, authorship, and/or publication of this article: This study was supported by the Saitama Prefectural University Incentive Research Grant (grant no. A-1) and the Japanese Non-surgical Orthopedics Society (JNOS) (grant no. JNOS 202005).

ORCID ID

Takuma Kano  <https://orcid.org/0000-0001-7619-513X>

REFERENCES

- Dunn WR, Lyman S, Lincoln AE, Amoroso PJ, Wickiewicz T, Marx RG. The effect of anterior cruciate ligament reconstruction on the risk of knee reinjury. *Am J Sports Med* 2004;**32**:1906–14
- Gornitzky AL, Lott A, Yellin JL, Fabricant PD, Lawrence JT, Ganley TJ. Sport-specific yearly risk and incidence of anterior cruciate ligament tears in high school athletes: a systematic review and meta-analysis. *Am J Sports Med* 2016;**44**:2716–23
- Amiel D, Billings E Jr, Harwood FL. Collagenase activity in anterior cruciate ligament: protective role of the synovial sheath. *J Appl Physiol* 1990;**69**:902–6
- Attia E, Brown H, Henshaw R, George S, Hannafin JA. Patterns of gene expression in a rabbit partial anterior cruciate ligament transection model: the potential role of mechanical forces. *Am J Sports Med* 2010;**38**:348–56
- Bray RC, Leonard CA, Salo PT. Correlation of healing capacity with vascular response in the anterior cruciate and medial collateral ligaments of the rabbit. *J Orthop Res* 2003;**21**:1118–23
- Woo SL, Young EP, Ohland KJ, Marcin JP, Horibe S, Lin HC. The effects of transection of the anterior cruciate ligament on healing of the medial collateral ligament. A biomechanical study of the knee in dogs. *J Bone Joint Surg Am* 1990;**72**:382–92
- Menetrey J, Laumonier T, Garavaglia G, Hoffmeyer P, Fritschy D, Gabbiani G, Bochaton-Piallat ML. α -Smooth muscle actin and TGF- β receptor I expression in the healing rabbit medial collateral and anterior cruciate ligaments. *Injury* 2011;**42**:735–41
- Murray MM, Fleming BC. Biology of anterior cruciate ligament injury and repair: Kappa Delta Ann Doner Vaughn award paper 2013. *J Orthop Res* 2013;**31**:1501–6
- Woo SL, Inoue M, McGurk-Burleson E, Gomez MA. Treatment of the medial collateral ligament injury: II: structure and function of canine knees in response to differing treatment regimens. *Am J Sports Med* 1987;**15**:22–9
- Kessler MA, Behrend H, Henz S, Stutz G, Rukavina A, Kuster MS. Function, osteoarthritis and activity after ACL-rupture: 11 Years follow-up results of conservative versus reconstructive treatment. *Knee Surg Sports Traumatol Arthrosc* 2008;**16**:442–8
- Kano T, Kokubun T, Murata K, Oka Y, Ozone K, Arakawa K, Morishita Y, Takayanagi K, Kanemura N. Influence of the site of injury on the spontaneous healing response in a rat model of total rupture of the anterior cruciate ligament. *Connect Tissue Res* 2022;**63**:138–50
- Kokubun T, Kanemura N, Murata K, Moriyama H, Morita S, Jinno T, Ihara H, Takayanagi K. Effect of changing the joint kinematics of knees with a ruptured anterior cruciate ligament on the molecular biological responses and spontaneous healing in a rat model. *Am J Sports Med* 2016;**44**:2900–10
- Morishita Y, Kanemura N, Kokubun T, Murata K, Takayanagi K. Acute molecular biological responses during spontaneous anterior cruciate ligament healing in a rat model. *Sport Sci Health* 2019;**15**:659–66
- Nishikawa Y, Kokubun T, Kanemura N, Takahashi T, Matsumoto M, Maruyama H, Takayanagi K. Effects of controlled abnormal joint movement on the molecular biological response in intra-articular tissues during the acute phase of anterior cruciate ligament injury in a rat model. *BMC Musculoskelet Disord* 2018;**19**:175
- Ihara H, Kawano T. Influence of age on healing capacity of acute tears of the anterior cruciate ligament based on magnetic resonance imaging assessment. *J Comput Assist Tomogr* 2017;**41**:206–11
- Ihara H, Miwa M, Takayanagi K, Nakayama A. Acute torn meniscus combined with acute cruciate ligament injury. *Clin Orthop Relat Res* 1994:146–54
- Yuge S, Nishiyama K, Arima Y, Hanada Y, Oguri-Nakamura E, Hanada S, Ishii T, Wakayama Y, Hasegawa U, Tsujita K, Yokokawa R, Miura T, Itoh T, Tsujita K, Mochizuki N, Fukuhara S. Mechanical loading of intraluminal pressure mediates wound angiogenesis by regulating the TOCA family of F-BAR proteins. *Nat Commun* 2022;**13**:2594
- Zhang F, Liu H, Stile F, Lei MP, Pang Y, Oswald TM, Beck J, Dorsett-Martin W, Lineaweaver WC. Effect of vascular endothelial growth factor on rat Achilles tendon healing. *Plast Reconstr Surg* 2003;**112**:1613–9
- Shook BA, Wasko RR, Mano O, Rutenberg-Schoenberg M, Rudolph MC, Zirak B, Rivera-Gonzalez GC, López-Giráldez F, Zarini S, Rezza A, Clark DA, Rendl M, Rosenblum MD, Gerstein MB, Horsley V. Dermal adipocyte lipolysis and myofibroblast conversion are required for efficient skin repair. *Cell Stem Cell* 2020;**26**:880–956
- Faryniarz DA, Chaponnier C, Gabbiani G, Yannas IV, Spector M. Myofibroblasts in the healing lapine medial collateral ligament: possible mechanisms of contraction. *J Orthop Res* 1996;**14**:228–37
- Serini G, Gabbiani G. Mechanisms of myofibroblast activity and phenotypic modulation. *Exp Cell Res* 1999;**250**:273–83
- Morito T, Muneta T, Hara K, Ju YJ, Mochizuki T, Makino H, Umezawa A, Sekiya I. Synovial fluid-derived mesenchymal stem cells increase after intra-articular ligament injury in humans. *Rheumatology* 2008;**47**:1137–43
- He X, Dong Z, Cao Y, Wang H, Liu S, Liao L, Jin Y, Yuan L, Li B. MSC-derived exosome promotes M2 polarization and enhances cutaneous wound healing. *Stem Cells Int* 2019;**2019**:7132708
- Toy BJ, Yeasting RA, Morse DE, McCann P. Arterial supply to the human anterior cruciate ligament. *J Athl Train* 1995;**30**:149–52
- Murray MM, Bennett R, Zhang X, Spector M. Cell outgrowth from the human ACL in vitro: regional variation and response to TGF- β 1. *J Orthop Res* 2002;**20**:875–80
- Murata K, Kanemura N, Kokubun T, Fujino T, Morishita Y, Onitsuka K, Fujiwara S, Nakajima A, Shimizu D, Takayanagi K. Controlling joint instability delays the degeneration of articular cartilage in a rat model. *Osteoarthritis Cartilage* 2016;**25**:297–308
- Geiger MH, Green MH, Monosov A, Akeson WH, Amiel D. An in vitro assay of anterior cruciate ligament (ACL) and medial collateral ligament (MCL) cell migration. *Connect Tissue Res* 1994;**30**:215–24
- Murakami H, Shinomiya N, Kikuchi T, Yoshihara Y, Nemoto K. Upregulated expression of inducible nitric oxide synthase plays a key role in early apoptosis after anterior cruciate ligament injury. *J Orthop Res* 2006;**24**:1521–34
- Nagineni CN, Amiel D, Green MH, Berchuck M, Akeson WH. Characterization of the intrinsic properties of the anterior cruciate and medial collateral ligament cells: an in vitro cell culture study. *J Orthop Res* 1992;**10**:465–75
- Xie J, Huang W, Jiang J, Zhang Y, Xu Y, Xu C, Yang L, Chen PC, Sung KL. Differential expressions of lysyl oxidase family in ACL and MCL fibroblasts after mechanical injury. *Injury* 2013;**44**:893–900

(Received May 10, 2023, Accepted October 12, 2023)